Reactive and Functional Polymers 93 (2015) 156–162

Contents lists available at ScienceDirect

Reactive and Functional Polymers

journal homepage: www.elsevier.com/locate/react

Photoprotective effect of starch/montmorillonite composites on ultraviolet-induced degradation of herbicides

Amanda S. Giroto [a], Adriana de Campos [b], Elaine I. Pereira [b], Tatiana S. Ribeiro [c], José M. Marconcini [b], Caue Ribeiro [b,*]

[a] Federal University of São Carlos, Department of Chemistry, Washington Luiz Highway, km 235, Zip Code: 13565-905 São Carlos, SP, Brazil
[b] Embrapa Instrumentation, 1452, XV de Novembro Street, CP: 741, Zip Code: 13560-970 São Carlos, SP, Brazil
[c] Federal University of São Carlos, Department of Natural Sciences, Mathematics and Education, Anhanguera Highway Km 174, Zip Code: 3600-970 Araras, SP, Brazil

ARTICLE INFO

Article history:
Received 20 February 2015
Received in revised form 10 June 2015
Accepted 17 June 2015
Available online 19 June 2015

Keywords:
Biocomposites
Herbicide
Photostability
Thermal stability

ABSTRACT

Despite the extensive research about polymer/clay composites and nanocomposites, there have been few investigations devoted to the resistance of these hybrids against ultraviolet radiation. This property is especially of interest for materials based on biodegradable polymers since they could be applied for slow release of light-degradable molecules, such as herbicides. This paper describes the photoprotective effect of starch/montmorillonite composites on the ultraviolet-induced degradation of ametryne, a commercial herbicide. The starch/montmorillonite composites highly loaded with ametryne (50% by weight), and different contents of clay were produced by the starch gelatinization method. The results showed that encapsulation of ametryne by starch/montmorillonite composites is simple and possible to be done as a one-step procedure. It was shown that the main photodegradation mechanism involves herbicide volatilization, which was significantly reduced due to formation of composites with starch and montmorillonite. The composite presented a synergistic photoprotective effect between components. ^{13}C solid-state nuclear magnetic resonance (^{13}C-NMR) and FTIR spectroscopy indicated that the photoprotective effect is based on absorption of ultraviolet radiation by starch/montmorillonite composites, and not due to herbicide interaction with the hybrid structure. The novel composites for controlled or slow delivery of herbicides exhibited a promising efficiency in protecting active inputs against solar light degradation in field.

1. Introduction

Herbicides have a singular importance in agricultural productivity due to their role in eliminating weeds in crops, which compete with plants for water, light, nutrients and space [1]. An ideal herbicide is one that remains active in the environment for a period of time sufficiently long to control the target weed, but not long enough to cause injuries to crops and environment [1,2]. The susceptibility or resistance of an herbicide against environmental degradation usually determines its residence time in a given culture, and thus its effectiveness in specific plantations [3]. The photostability of herbicides beneath ultraviolet (UV-C) radiation, for instance, is a key property to be controlled, and plays an important role in avoiding excessive and unnecessary application of herbicides in agriculture. Photodegradation is one of the most common degradation processes of pesticides [4]. The sunlight that reaches the surface of the earth contains UV-C rays (290–400 nm) which can degrade pesticides by direct photolysis and indirect photolysis [5–7]. In direct photolysis, the high-energy UV rays are directly absorbed by organic compounds, causing a chemical reaction. In indirect photolysis, the radiation is absorbed by photosensitizes solutes, resulting in the formation of reactive intermediates that react with the organic compounds [6]. As a result, the effect of pesticides on a target pest is diminished, and harmful photodegradation products might be formed and released to the environment [5,6].

Photodegradation of polymers (chain scission and/or crosslinking) is likely caused by activation of polymer macromolecules as a result of photon absorption. The control of this chemical phenomenon is of particular interest, since photodegradation has the potential of facilitating biodegradation by reducing molecular weight and introducing oxygen groups on polymer chain, which also facilitate further chemical degradation [3–10]. In this context, the use of biopolymers as protective agents – where they could serve as a matrix that encapsulates the active compound – has attracted much scientific attention [11–16]. The protective effect of biopolymers is mostly attributed to a sacrificial behavior, i.e., the material blocks ultraviolet radiation by suffering degradation, thereby decreasing the exposure of the active compound. This effect is thus limited, and may demand a large amount of biopolymer in order to achieve a proper final efficiency. On the other hand, inorganic materials may act as photoprotective agents by pathways involving reflection of incident radiation or excitation/decay of electronic levels [17]. Generally, a well-dispersed inorganic phase may reduce ultraviolet-induced

* Corresponding author.
E-mail address: caue.ribeiro@embrapa.br (C. Ribeiro).

http://dx.doi.org/10.1016/j.reactfunctpolym.2015.06.013
1381-5148/

reactions by absorbing part of the spectrum, avoiding transference of energy to the active compound. This effect may also be particularly useful in biopolymers, since the production of nanocomposites using inorganic phases (for instance, exfoliated clays) has been extensively reported in the last few decades [18,19]. However, to the best of our knowledge there are only few studies devoted to the photoprotective effect of dispersed clays on biopolymers and, specifically, their shielding effect when applied as a host matrix for light-degradable compounds, such as herbicides.

In this study starch/montmorillonite composites were prepared by the starch gelatinization method without the use of plasticizers, with the aim of serving as a host matrix to improve the photostability of ametryne, a commercial herbicide. Starch was chosen because it is an abundant, renewable, and biodegradable polymer obtained from many agricultural sources, thereby being convenient for scaled up applications [11,21–25]. Furthermore starch is a hydrophilic biopolymer, and montmorillonite readily suffers exfoliation in aqueous medium, then compatibilization between starch and montmorillonite was expected to occur spontaneously, without the use of compatibilizers [27,28]. Different factors affecting the photostability of the starch/montmorillonite/ametryne composites were examined. The discussion was based on structural, thermal, and spectroscopic characterizations of the composites before and after exposure to UV-C radiation.

2. Experimental

2.1. Materials

Ametryne (aqueous solution, Metrimex 500 SC) was supplied by Nufarm. Montmorillonite (Mt) (Bentonite, Drescon S/A) was purchased from Drilling Products, and regular corn starch (St) (Amidex 3001, 30% amylose and 70% amylopectin) was kindly supplied by Corn Products Brazil. All these materials were used as received.

2.2. Preparation of ametryne-loaded composites

Starch/montmorillonite composites were obtained by starch (St) gelatinization following the procedure described by Giroto et al. [26]. Briefly, starch was first dispersed into distilled water (5 wt.%) using mechanical stirring for 15 min, and then heating the dispersion to approximately 90 °C for 30 min until formation of a sticky starch gel. The temperature was then decreased to 70 °C and montmorillonite (Mt) was added to the gelatinized starch gel. Since Mt is dispersible in water, its compatibilization with starch gel was done by vigorous shaking in a similar manner as proposed by Valadares et al. [27] and Bragança et al. [28] for natural rubber nanocomposites. Ametryne (Amet) was added at a concentration of 50 wt.% (with basis on the total mass of the composite) to the starch gel simultaneously with Mt in order to accomplish encapsulation of the herbicide into the St/Mt composite structure. The gelatinized formulation was then stored at 50 °C into an air circulating oven for at least 72 h to obtain a dried solid material. All samples were prepared using the same procedure. The different ratios of St and Mt ($w \cdot w^{-1}$ basis) are listed in Table 1. All samples were dried at 50 °C and stored in dry boxes prior to characterizations. The final water content in the composites was approximately 4%.

Table 1
Mix design used in the production of composites.

Samples	Amount (g)			
Starch (St)	15	15	15	15
Montmorillonite (Mt)	0	15	30	60
Ametryne (Amet)	15	30	45	75
Designation	St/Amet 1:1	1:1:2 Amet	1:2:3 Amet	1:4:5 Amet

2.3. Experiments of degradation induced by UV-C radiation

Composites samples were exposed to UV-C radiation in a chamber (40 cm × 60 cm) set at constant temperature of 25 °C and relative humidity of 65%. Eight parallel tube lamps (16 W each) were positioned at the top of the chamber at a distance of 22 cm to the sample surface. The samples were irradiated continuously for 8 days [29] and the weight loss was monitored using an analytical scale. Afterwards, the samples were removed from the chamber, and characterized by means of scanning electron microscopy (SEM), X-ray diffraction (XRD), thermogravimetric analysis (TGA), infrared spectroscopy (FTIR) and solid state ^{13}C NMR spectroscopy (NMR). The parameters used for each technique are described hereafter. All irradiated samples were designated with the acronym (irr).

2.4. Characterizations

The morphology and relative element concentration of the samples were assessed by scanning electron microscopy (SEM) using a JSM 6510 microscope (JEOL) equipped with an EDX analysis system (Thermo Scientific NSS coupled or linked). Samples were previously fixed onto carbon tapes, and coated with thin layer of gold in an ionization chamber (BALTEC Med. 020). The imaging by SEM was carried out using the secondary electron mode. X-ray diffraction patterns were obtained on a Shimadzu XRD 6000 diffractometer using Cu Kα radiation (λ = 0.15405 nm). The measurements were performed using a scanning speed of $1°.min^{-1}$ in the 2θ range of 3–40°. The X-ray tube was excited with a voltage of 30 kV and current of 30 mA. Thermal degradation of samples was evaluated in the range 25 °C–600 °C using a Q500 analyzer (TA Instruments, New Castle, DE, USA) under the following conditions: sample size of 10.0 ± 0.5 mg, synthetic air atmosphere (80% N_2 and 20% O_2) with flow of 60 $mL.min^{-1}$, and heating rate of 10 $°C.min^{-1}$. The vibrational spectra were obtained with a Shimadzu FTIR-8300 spectrometer in the range 4000–400 cm^{-1}. KBr pellets were prepared by mixing 5 mg of sample with 200 mg of anhydrous KBr. Structural analyses were conducted by solid state ^{13}C NMR spectroscopy using a spectrometer Varian Inova 400 model (9.4 T). The ^{13}C-NMR spectra were obtained at ^{13}C core with the CPMAS technique and high-power decoupling under the following conditions: pulse of π/2 of 4 μm, contact time of 1 ms, 16,384 points, and repetition time of 3 s. Samples were measured in a 5 mm ZrO rotor, rotation in magic angle of 10 kHz, 2048 transients and lb = 20. The chemical shift values were calibrated using hexamethyl benzene (HMB) at 17.2 ppm.

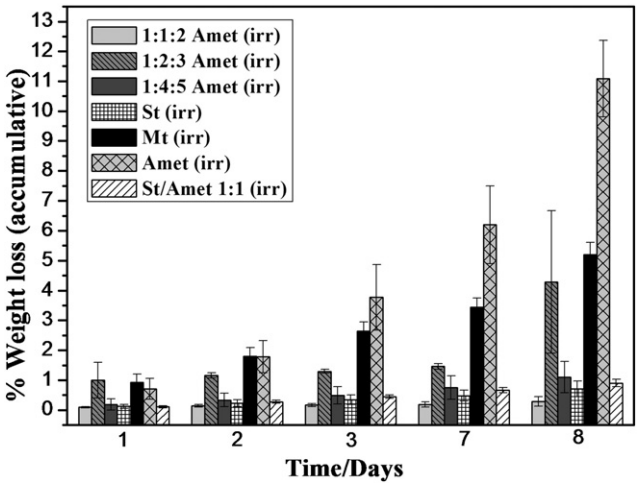

Fig. 1. Percentage of accumulative weight loss of samples exposed to ultraviolet (UV-C) radiation.

3. Results and discussion

The photodegradation of the St/Mt/Amet composites induced by UV-C radiation was initially evaluated by the variation of accumulated mass over exposure time, as shown in Fig. 1. It was observed that pure Amet suffered mass loss at the highest extent after three days of exposure to UV-C radiation. Moreover, a significant mass loss was observed for the St/Amet 1:1 sample only after seven days of treatment, whereas all the Mt-loaded composites had their mass practically unaltered. Possibly the St/Amet 1:1 sample presented disruption of its starch moiety, leading to an exposure of the encapsulated herbicide particles to UV-C radiation, and facilitating their release after some time. This became evident by the analysis of the photodegradation of pure starch gel which displayed intense mass loss after 8 days. However, it is noteworthy that the starch encapsulation process was effective in reducing Amet photodegradation. The protective effect of Mt on the composite photodegradation was found to be dependent on the clay content. The mass loss values decreased when the content of Mt in the St/Mt/Amet composites was increased.

SEM micrographs of the neat materials and all composite samples before and after exposure to UV-C radiation are depicted in Fig. 2. Starch gel was seen as a homogeneous material forming a thick polymeric structure (Fig. 2a). It was observed that neat starch gel presented superficial modifications after UV-C exposure, indicating some chemical scission of the starch polymer chains. It is suggested that the starch photo-oxidation starts by breaking of the C2–C3 bond of the glucopyranose ring, producing a starch dialdehyde, and then followed by the formation of formaldehyde, formic acid and CO_2 [30] (Fig. 2d). Amet was observed as rounded, micrometric particles, which suffered morphological changes over UV-C exposure time. This was revealed by the faceting of the Amet particles probably due to volatilization of the herbicide (Fig. 2e). Such a behavior was also observed by Wienhold et al. for atrazine herbicide particles after UV-C irradiation [31]. According to Lau et al. [32] the volatilization of metolachlor herbicide may occur at a temperature below its boiling point. Weight losses were observed at temperatures below its boiling temperature. This behavior was explained by the increase of Henry's constant with increasing temperature [23,24,30–32]. As expected, morphological changes in Mt particles after

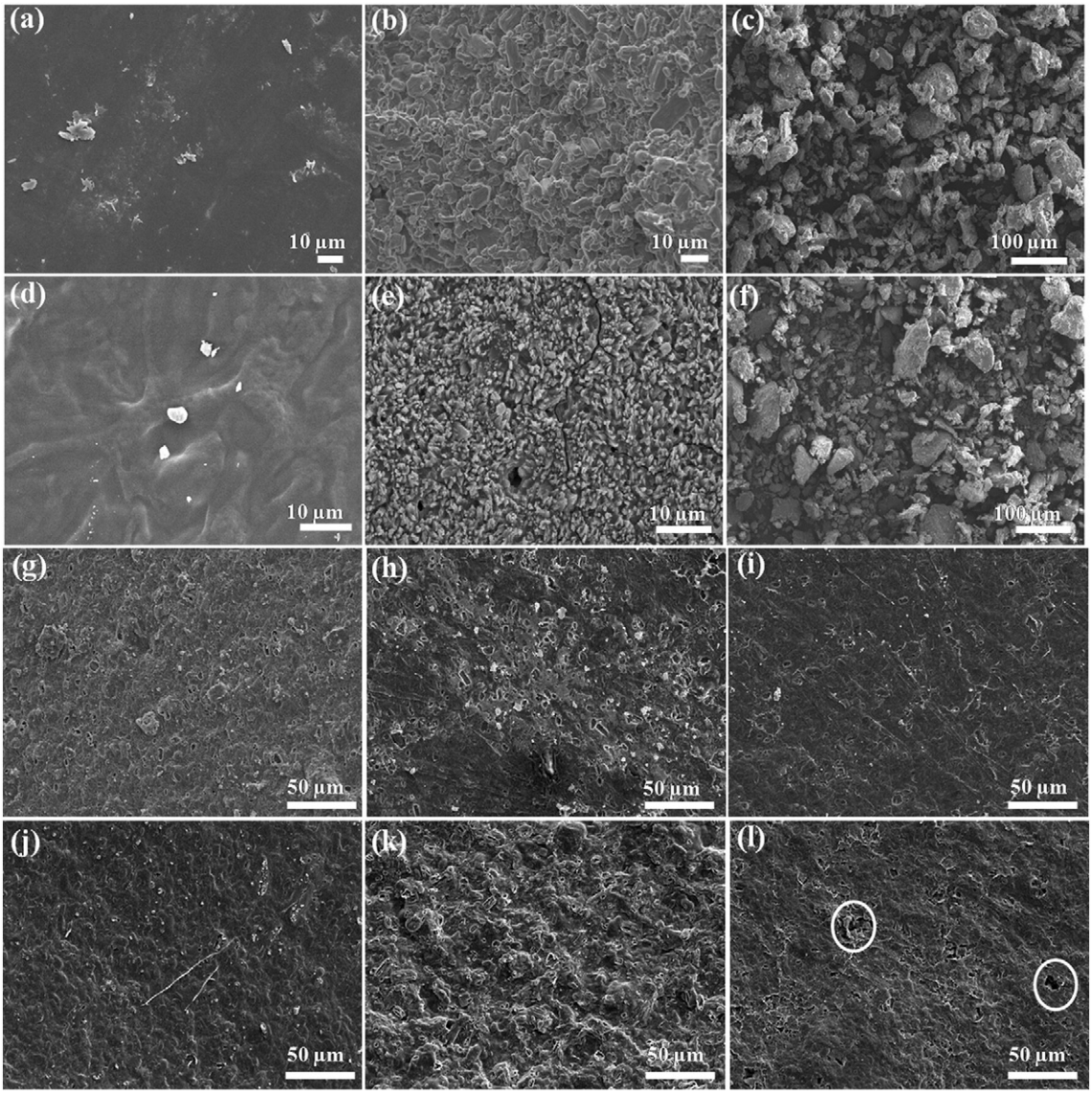

Fig. 2. SEM micrographs of neat components before (a) St, (b) Amet, (c) Mt, and after (d) St(irr), (e) Amet(irr), (f) Mt(irr) UV-C irradiation, and their analogous composites before (g) 1:1:2 Amet, (h) 1:2:3 Amet, (i) 1:4:5 Amet and after (j) 1:1:2 Amet(irr), (k) 1:2:3 Amet(irr), (l) 1:4:5 Amet(irr) exposure to UV-C radiation.

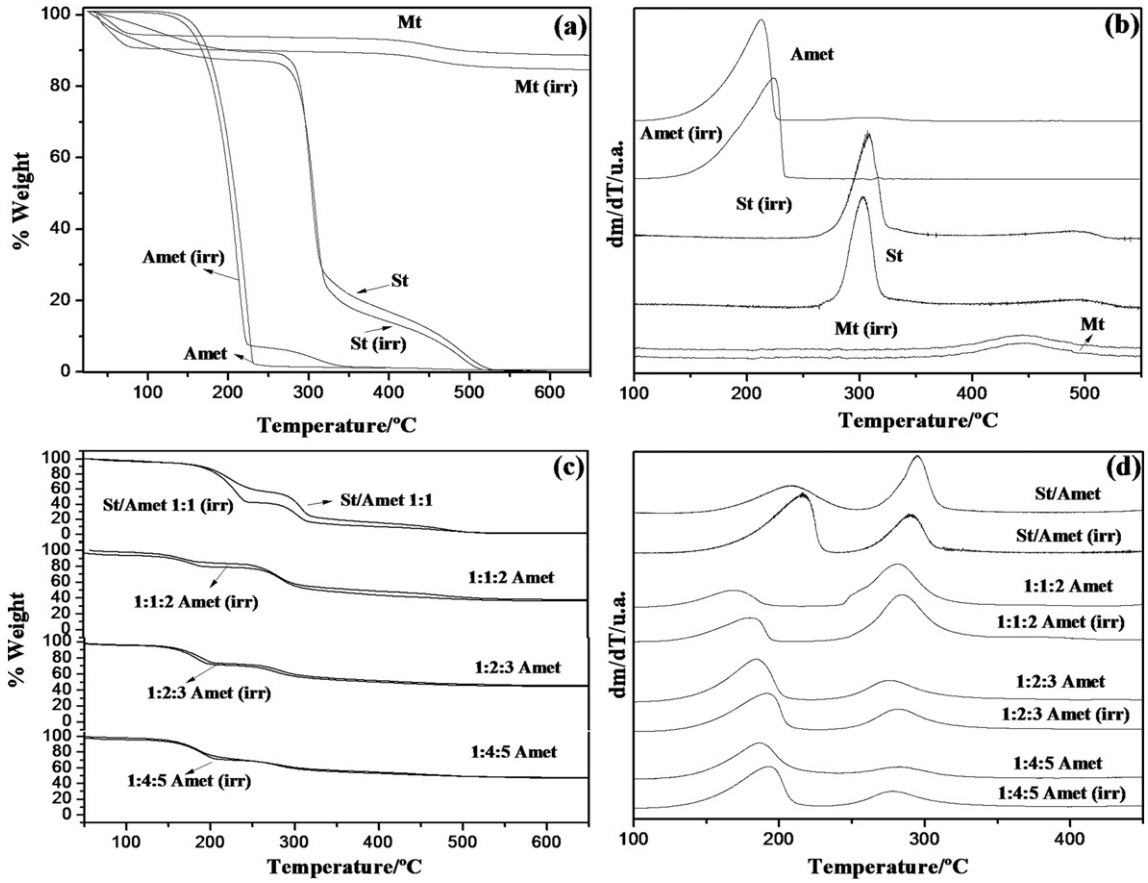

Fig. 3. (a) TG curves and (b) DTG curves of (St, Mt and Amet) and after UV-C irradiation (St(irr), Mt(irr) and Amet(irr)); (c) TG curves and (d) DTG curves of St/Mt/Amet composites before and after UV-C irradiation.

irradiation were not observed by SEM (Fig. 2f), once the clay is capable of absorbing light [23].

Likewise, it was not verified by any morphological change in all Mt-loaded composites after UV-C exposure. It is suggested that the light absorption capability of Mt was preserved after the formation of composites with St and Amet, thus avoiding photoexcitation of Amet. The Mt particles might also had acted as acceptors of excess energy from the surrounding molecules by energy transfer or energy charge transfer mechanisms, dissipating this energy through their surface and diminishing the herbicide degradation [22]. As a result, the residence time of Amet in the St/Mt composites was substantially increased. However, St/Mt/Amet 1:4:5 had the highest concentration of Mt, and there was some phase segregation and unprotected regions in this sample that could have suffered photodegradation. These regions presented voids probably due to the release of small amounts of herbicide, as emphasized in Fig. 2l. These results indicated that Mt threshold induced phase segregation within the composite structure, leading to a decrease of the shielding effect of Mt for the Amet-loaded composites.

Fig. 3 shows the thermal profiles of the neat materials and composites submitted to UV irradiation. Mt presented a weight loss of 10% after exposure which can be ascribed to water release (Fig. 3a) [33]. UV-C irradiated neat St gel and Amet, St(irr) and Amet(irr) respectively,

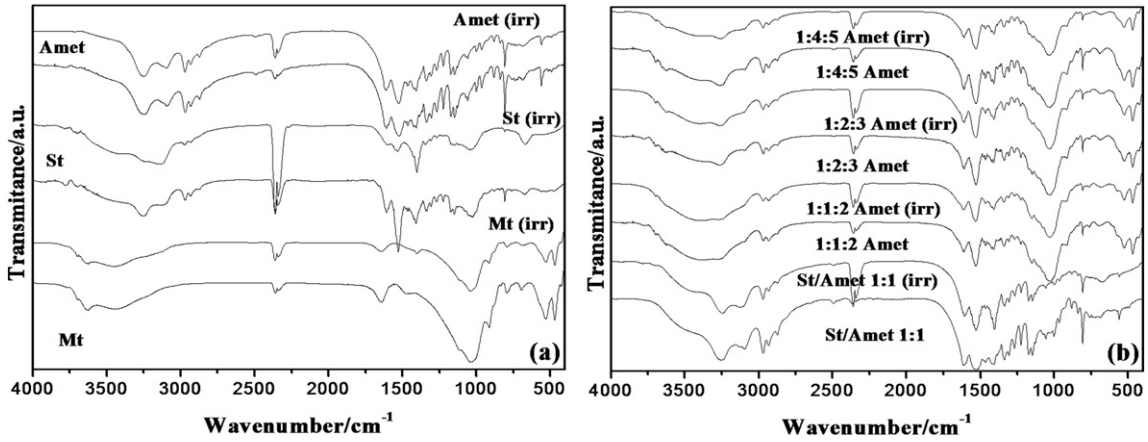

Fig. 4. (a) FTIR spectra of neat precursors before (St, Mt and Amet) and after (St(irr), Mt(irr) and Amet(irr)) UV-C exposure; (b) FTIR spectra of St/Amet 1:1, 1:1:2 Amet, 1:2:3 Amet and 1:4:5 Amet before and after 8 days of UV-C irradiation.

presented a slight mass loss, however, a decreased thermal stability was observed for these samples if compared to their non-irradiated counterparts. The initial temperature of thermal degradation for Amet(irr) was shifted from 230 °C to 180 °C, while for St(irr) gel the shift was from 300 °C to 290 °C. This suggests that the irradiated St(irr) gel suffered a structural collapse, creating voids that facilitated Amet volatilization (Fig. 3b). These results were in accordance with the SEM measurements. The St/Mt/Amet composites presented three stages of mass loss (Fig. 3c). The first stage is related to water release and Amet degradation. The second stage is ascribed to the degradation of St, and the third stage corresponds to the dehydroxylation of Mt. It can be noted that the thermal degradation of irradiated St/Amet 1:1 started at temperatures lower than those of its non-irradiated counterpart (210 °C). This can be ascribed to the Amet volatilization. The irradiated St/Mt/Amet composites (1:1:2, 1:2:3 and 1:4:5 Amet) exhibited an increased thermal stability with relation to the first stage of decomposition when compared with the non-irradiated composite samples. It has been found that inorganic nanoparticles, such as SiO_2, Al_2O_3 and ZnO can effectively improve photo-stability of composite materials [18-20]. Chiou et al. [21] reported that St/Mt composites presented an improved thermal stability due to the nanoclay function as a structural barrier against diffusion of volatile compounds formed during starch decomposition. Exfoliation of nanoclays was also found to impart higher thermal stability to starch in comparison with intercalated nanoclays [29].

FTIR and XRD measurements were performed in order to detect chemical and structural changes in the St/Mt/Amet composites. Fig. 4a displays the FTIR spectra of St, Amet and Mt before and after UV-C irradiation. The St(irr) sample presented a vibration band at 3780 cm^{-1} attributed to the stretching O–H. New vibration bands were also observed at 3110 cm^{-1} and 3247 cm^{-1} attributed to stretching O–H and increase of intermolecular hydrogen bonding, respectively. The band at 2924 cm^{-1} ascribed to the stretching C–H was shifted to 2970 cm^{-1}. The band at 1645 cm^{-1} ascribed to water molecules bonded to the amorphous domains of St was also verified to shift to 1610 cm^{-1} after irradiation [17]. The spectrum of Amet(irr) presented a decrease in the intensity of the vibration band between 3500 and 3000 cm^{-1} related to stretching N–H. Mt did not show changes in its FTIR spectrum after UV-C irradiation, except an increase of intensity for the vibration band at 3460 cm^{-1} related to stretching O–H. This was an indicative of release of interlamellar water rather than the collapse of the Mt lamellar structure. It is supposed that the interlamellar water molecules experienced higher mobility into the Mt galleries after UV-C irradiation. Fig. 4b presents the FTIR spectra of irradiated and non-irradiated St/Mt/Amet composites. The spectrum of the St/Amet 1:1 sample after UV-C exposure showed a displacement of the band at around 3019–3120 cm^{-1}. The St vibration bands overlapped the Amet vibration bands in the spectral region between 1600 cm^{-1} and 1250 cm^{-1}. It emphasizes the hypothesis that the structural collapse of the St moiety in this sample exposed the Amet particles and facilitated their volatilization. A different behavior was observed in the composite spectra. For these samples, it only observed a decrease of intensity of the stretching O–H vibration band because of the minor loss of moisture. This confirms the photoprotective effect of Mt on the composites submitted to UV-C irradiation [29].

XRD patterns displayed in Fig. 5a were collected to verify changes in the crystallinity and properties of the composites after UV-C irradiation. It can be seen that the crystallinity of the pure St gel was slightly modified after exposure to UV-C (Fig. 5a). It was also shown by XRD two low intensity peaks, indicating incomplete gelatinization of St. Nevertheless, the macromolecular organization of St was more affected after UV-C treatment, indicating retrogradation. The photo-degradation of St induced by UV-C radiation is limited to occur at the amorphous domains of St. The XRD patterns of the native starch granules and the St(irr) gel were compared in an attempt to examine whether UV-C irradiation provoked re-crystallization of the starch matrix. It was observed that the irradiated sample presented peaks similar to those seen in the native starch pattern. This indicated that St(irr) gel suffered retrogradation, leading to an increase of crystallinity in this sample. Irradiated Mt did not show modification in the d_{001} basal spacing (Fig. 5b). This result suggested that the interlamellar water released during UV-C irradiation did not alter the layered structure of Mt. Amet(irr) and was slightly less crystalline than the neat herbicide samples, which was seen by the reflections between 8° and 16° of 2θ (Fig. 5b). The same effect is perceptible for St/Amet 1:1 after UV-C irradiation. This indicates that similar

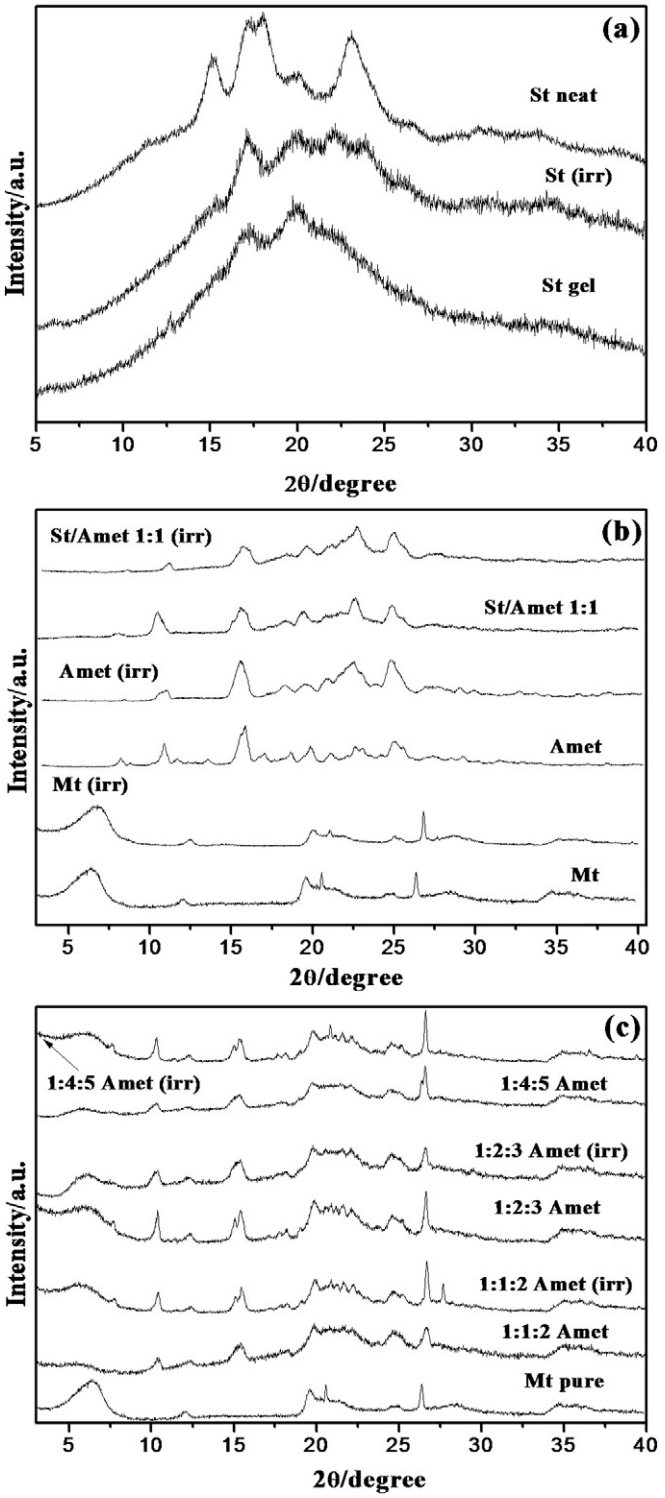

Fig. 5. X-ray diffraction patterns of (a) neat St, St(irr) and St; (b) Mt, Amet, and their corresponding irradiated counterparts; (c) 1:1:2 Amet, 1:2:3 Amet, 1:4:5 Amet before and after exposure to UV-C radiation.

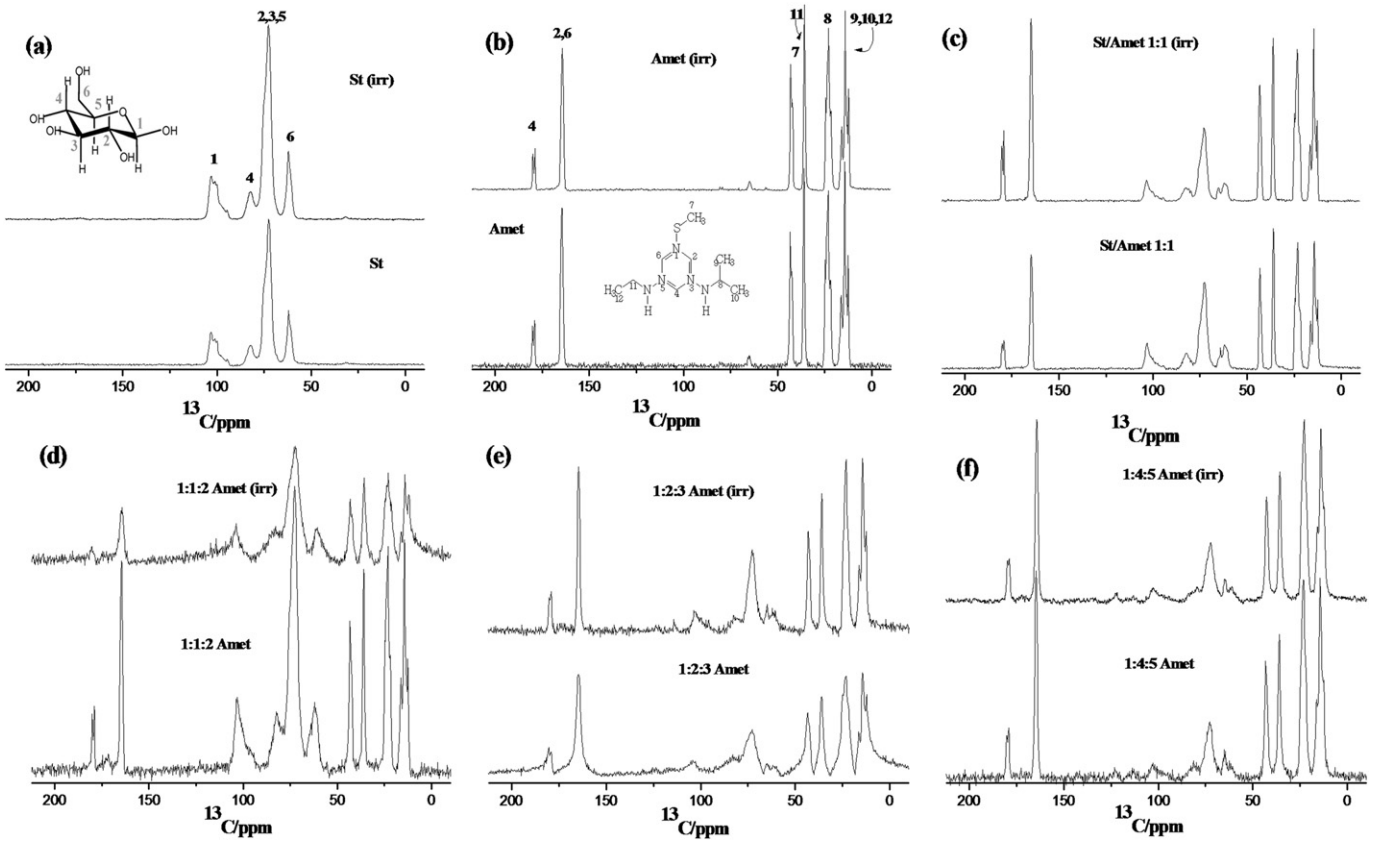

Fig. 6. ^{13}C CP/MAS NMR spectra of (a) St, (b) Amet, (c) St/Amet 1:1; (d) 1:1:2 Amet; (e) 1:2:3 Amet; (f) non-irradiated (1:4:5 Amet) and irradiated (1:4:5 Amet(irr)).

amorphization might have occurred in this sample. On the other hand, the XRD patterns for all St/Mt/Amet composites (Fig. 5c) before and after irradiation were very similar, showing that the presence of Mt efficiently reduced the amorphization process. It was also seen that the St/Mt/Amet composites presented a rearrangement of the basal peak at 6.6° of 2θ (Fig. 5c) probably due to the release of water induced by the UV-C exposure. A similar result was observed by Lombardo et al. [34] in poly(ethylene oxide)/Mt nanocomposites. The authors also observed that Mt not only scattered the incident UV-C radiation but also absorbed it, thereby minimizing the degradation rate of the nanocomposites.

^{13}C NMR spectra were collected in order to elucidate the chemical interactions occurring between the Amet and the composite components. Fig. 6 displays the ^{13}C NMR spectra of neat St, Amet and composites loaded with different contents of Mt. The glucose spectrum ($C_6H_{12}O_6$) was used as a reference for St, since it is a homopolymer of glucose. The St spectrum showed four signals referent to a chemical shift (Fig. 6a). The signal observed at δ 103.3 ppm is attributed to C-1 and the signal observed at δ 72.7 ppm is attributed to the C-2, C-3 and C-5 of the starch structure. The signals at δ 82.5 ppm and δ 62.1 ppm are attributed to C-4 and C-6, respectively [34–37]. Fig. 6a shows wider variations in the chemical shift of C-4 and C-6 after the incorporation of Mt within the St gel structure. The chemical shifts of these samples have been summarized in Table 2.

The Amet ^{13}C NMR spectrum shows eight chemical shift signals. The signals at δ 14 ppm and δ 43.5 ppm were assigned to the aliphatic part, and the signals at δ 164.4 ppm and δ 179.7 ppm were assigned to the aromatic part of the herbicide molecule. The St/Amet 1:1 sample did not present a significant chemical shift probably due to a weak interaction between the St and Amet functional groups. A significant chemical shift in the Amet signals was not observed considering the different St/Mt ratios used in the composites.

The aliphatic groups of C-9, C-10 and C-12 presented some minor shift, indicating that chemical interactions were formed between Amet and the composite structure through lateral groups of Amet and hydroxyl groups of the St polymer chains. However, when compared with the chemical shift observed in the composites with different Mt contents, there were higher chemical shifts for all carbons attached to the hydroxyl groups, suggesting hydrophilic interaction between St and Mt. This finding is in agreement with the FTIR result presented in Fig. 4b.

The ^{13}C NMR spectra of the irradiated St/Mt/Amet composites did not present significant chemical shifts. This confirms that Mt protected the herbicide against photo-degradation. Mt has been used as a catalyst for degradation of organic compounds, but in this study it was found that this catalytic activity was less important or absent than the Mt photo-protective effect.

Table 2
Chemical shift of ^{13}C CP/MAS NMR spectra in solid state (δ ^{13}C/ppm) of neat starch and starch intercalated with montmorillonite.

δ ^{13}C of starch gel				
Materials	C-1	C-4	C-2, C-3 and C-5	C-6
St	103.3	82.5	72.7	62.1
$St_{(i)}$	103.4	82.5	72.7	61.9
St/Amet 1:1	103.1	83.0	72.7	62.1
St/Amet $1:1_{(i)}$	103.1	82.0	72.7	62.4
1:1:2 Amet	103.6	81.8	72.7	62.0
1:1:2 $Amet_{(i)}$	103.6	81.0	72.9	61.7
1:2:3 Amet	103.1	80.8	72.7	61.7
1:2:3 $Amet_{(i)}$	103.6	83.0	72.9	62.1
1:4:5 Amet	102.9	82.0	73.9	62.6
1:4:5 $Amet_{(i)}$	102.9	79.3	72.7	61.2

4. Conclusions

The encapsulation of ametryne by starch/montmorillonite composites is an effective strategy to protect herbicides against the influence of UV-C radiation. The presence of Mt in starch/ametryne 1:1 formulations at different contents imparted a photoprotective effect, absorbing UV-C radiation, thus avoiding the herbicide photodegradation. Suitable properties such as better thermal stability were also obtained. This study proposed a novel material for controlled or slow delivery of herbicides with the additional capability of protecting active inputs efficiently against solar degradation in field.

Acknowledgment

The authors are grateful to Embrapa-Brazil, FAPESP, CNPq, and CAPES for the financial support to this work.

References

[1] B. Singh, D.K. Sharma, R. Kumar, A. Gupta, Controlled release of the fungicide thiram from starch–alginate–clay based formulation, Appl. Clay Sci. 45 (2009) 76–82.
[2] M. Fernández-Pérez, F. Flores-Céspedes, E. González-Pradas, M. Villafranca-Sánchez, S. Pérez-García, F.J. Garrido-Herrera, Use of activated bentonites in controlled-release formulations of atrazine, J. Agric. Food Chem. 52 (2004) 3888–3893.
[3] Z. Gerstl, A. Nasser, U. Mingelgrin, Controlled release of pesticides into water from clay–polymer formulations, J. Agric. Food Chem. 46 (1998) 3803–3809.
[4] P. Liu, Y. Liu, Q. Liu, J. Liu, Photodegradation mechanism of deltamethrin and fenvalerate, J. Environ. Sci. 22 (2010) 1123–1128.
[5] O. Tiryyaki, C. Temur, The fate of pesticide in environment, J. Biol. Environ. Sci. 4 (2010) 29–38.
[6] M. Franko, M. Sarakha, A. Čibej, A. Boškin, M. Bavcon, P. Trebše, Photodegradation of pesticides and application of bioanalytical methods for their detection, Pure Appl. Chem. 77 (2005) 1727–1736.
[7] L. Margulies, H. Rozen, E. Cohen, Photostabilization of anitromethylene heterocycle insecticide on the surface of montmorillonite, Clays Clay Miner. 36 (1988) 159–164.
[8] D.F. Wallace, H.L. Hand, R.G. Oliver, The role of indirect photolysis in limiting the persistence crop protection products in surface waters, Environ. Toxicol. Chem. 29 (2010) 575–581.
[9] H.M. Nguyen, I.-C. Hwang, J.-W. Park, H.-J. Park, Photoprotection for deltamethrin using chitosan-coated beeswax solid lipid nanoparticles, Pest Manag. Sci. 68 (2012) 1062–1068.
[10] R.L. Shogren, J.W. Lawton, W.M. Doanne, F.K. Tiefenbacher, Structure and morphology of baked starch foams, Polymer 39 (1998) 6649–6655.
[11] A.E.S. Vercelheze, F.M. Fakhouri, L.H. Dall'Antônia, A. Urbano, E.Y. Youssef, F. Yamashita, S. Mali, Properties of baked foams based on cassava starch, sugarcane bagasse fibers and montmorillonite, Carbohydr. Polym. 87 (2012) 1302–1310.
[12] M.E. Carr, R.E. Wing, W.M. Doane, Encapsulation of atrazine within a starch matrix by extrusion processing, Cereal Chem. 68 (1992) 262–266.
[13] A. Chevillard, H. Angellier-Coussy, V. Guillard, N. Ontard, E. Gastaldi, Controlling pesticide release via structuring agropolymer and nanoclays based materials, J. Hazard. Mater. 205 (2012) 32–39.
[14] R. Grillo, N.Z.P. Santos, C.R. Maruyama, A.H. Rosa, R. Lima, L.F. Fraceto, Poly(ε-caprolactone) nanocapsules as carrier systems for herbicides: physico-chemical characterization and genotoxicity evaluation, J. Hazard. Mater. 15 (2012) 1–9.
[15] H. Guan, D. Chi, J. Yu, H. Li, Encapsulated ecdysone by internal gelation of alginate microspheres for controlling its release and photostability, Chem. Eng. J. 168 (2011) 94–101.
[16] J. Jerobin, R.S. Sureshkumar, C.H. Anjali, A. Mukherjee, N. Chandrasekaran, Biodegradable polymer based encapsulation of neem oil nanoemulsion for controlled release of Aza-A, Carbohydr. Polym. 90 (2012) 1750–1756.
[17] N. Muro-Suñé, R. Gani, G. Bell, I. Shirley, Predictive property models for use in design of controlled release of pesticides, Fluid Phase Equilib. 228 (2005) 127–133.
[18] A. Copinet, C. Bertrand, A. Longieras, V. Coma, Y. Couturier, Photodegradation and biodegradation study of a starch and poly(lactic acid) coextruded material, J. Polym. Environ. 11 (2003) 169–179.
[19] I. Grigoriadou, K.M. Paraskevopoulos, K. Chrissafis, E. Pavlidou, T.-G. Stamkopoulos, D. Bikiaris, Effect of different nanoparticles on HDPE UV stability, Polym. Degrad. Stab. 96 (2011) 151–163.
[20] V.R. Mendonça, C. Ribeiro, Influence of TiO_2 morphological parameters in dye photodegradation: a comparative study in peroxo-based synthesis, Appl. Catal. B Environ. 105 (2011) 298–305.
[21] B.-S. Chiou, D. Wood, E. Yee, S.H. Imam, G.M. Glenn, W.J. Orts, Extruded starch–nanoclay nanocomposites: effects of glycerol and nanoclay concentration, Polym. Eng. Sci. 47 (2007) 1898–1904.
[22] B. Ayana, S. Supratim, B.B. Khatua, Highly exfoliated eco-friendly thermoplastic starch (TPS)/poly(lacticacid)(PLA)/clay nanocomposites using unmodified nanoclay, Carbohydr. Polym. 110 (2014) 430–439.
[23] Y. El-Nahhal, S. Nir, L. Margulies, B. Rubin, Reduction of photodegradation and volatilization of herbicides in organo-clay formulations, Appl. Clay Sci. 14 (1999) 105–119.
[24] R. Kizil, J. Irudayaraj, K. Seetharaman, Characterization of irradiated starches by using FT-Raman and FTIR spectroscopy, J. Agric. Food Chem. 50 (2002) 3912–3918.
[25] T. Qilong, K.K.Y. Richard, S. Lei, H. Yuan, A novel polymeric flame retardant and exfoliated clay nanocomposites: preparation and properties, Chem. Eng. J. 183 (2012) 542–549.
[26] A.S. Giroto, A. Campos, E.I. Pereira, C.C.T. Cruz, J.M. Marconcini, C. Ribeiro, Study of a nanocomposite starch–clay for slow-release of herbicides: evidence of synergistic effects between the biodegradable matrix and exfoliated clay on herbicide release control, J. Appl. Polym. Sci. 121 (2014) 41188.
[27] L.F. Valadares, C.A.P. Leite, F. Galembeck, Preparation of natural rubber–montmorillonite nanocomposite in aqueous medium: evidence for polymer-platelet adhesion, Polymer (Guildford) 47 (2006) 672–678.
[28] F.C. Bragança, L.F. Valadares, C.A.P. Leite, F. Galembeck, Counterion effect on the morphological and mechanical properties of polymer–clay nanocomposites prepared in an aqueous medium, Chem. Mater. 19 (2007) 3334–3342.
[29] A. Campos, J.M. Marconcini, S.M. Martins-Franchetti, L.H.C. Mattoso, The influence of UV-C irradiation on the properties of thermoplastic starch and polycaprolactone biocomposite with sisal bleached fibers, Polym. Degrad. Stab. 97 (2012) 1948–1955.
[30] A. Bertolini, C. Mestres, J. Raffi, A. Buleon, D. Lerner, P. Colonna, Photodegradation of cassava and corn starches, J. Agric. Food Chem. 49 (2001) 675–682.
[31] B.J. Wienhold, A.M. Sadeghi, T.J. Gish, Effect of starch encapsulation and temperature on volatilization of atrazine and alachlor, J. Environ. Qual. 22 (1993) 162–166.
[32] Y.L. Lau, D.L.S. Liu, G.J. Pacepavicius, R.J. Maguire, Volatilization of metolachlor from water, J. Environ. Sci. Health 30 (1995) 605–620.
[33] M. Alboofetileh, M. Rezaei, H. Hosseini, M. Abdollahi, Effect of montmorillonite clay and biopolymer concentration on the physical and mechanical properties of alginate nanocomposite films, J. Food Eng. 117 (2013) 26–33.
[34] P.C. Lombardo, A.L. Poli, M.G. Neumann, D.S. Machado, C.C. Schmitt, Photodegradation of poly(ethyleneoxide)/montmorillonite composite films, J. Appl. Polym. Sci. 127 (2013) 3687–3692.
[35] J.K. Pandey, K.R. Reddy, A.P. Kumar, R.P. Singh, An overview on the degradability of polymer nanocomposites, Polym. Degrad. Stab. 88 (2005) 234–250.
[36] Y. Tozuka, A. Takeshita, A. Nagae, A. Wongmekiat, K. Moribe, T. Oguchi, Specific inclusion mode of guest compounds in the amylose complex analyzed by solid state NMR spectroscopy, Chem. Pharm. Bull. 54 (2006) 1097–1101.
[37] H.M. Wilhelm, M.R. Sierakowski, G.P. Souza, F. Wypych, The influence of layered compounds on the properties of starch/layered compound composites, Polym. Int. 52 (2003) 1035–1044.